

# Dynamic Analysis for Golf Swing using of Mode Synthetics Method for Suggesting an Optimal Club

Kenta Matsumoto<sup>1</sup>, Nobutaka Tsujiuchi<sup>1</sup>, Takayuki Koizumi<sup>1</sup>, Akihito Ito<sup>1</sup>,  
Masahiko Ueda<sup>2</sup> and Kosuke Okazaki<sup>2</sup>

<sup>1</sup>Department of Mechanical Engineering, Doshisha University, 1-3, Tataramiyakodani, Kyotanabe-city,  
Kyoto, 610-0321, Japan

<sup>2</sup>Research Dept. II, Research & Development HQ, Sumitomo Rubber Industries, Ltd, 1-1, 2-chome,  
Tsutsui-cho, Chuo-ku, Kobe 651-0071, Japan

Keywords: Golf Club, Finite Element Method, Mode Synthetics Method, Inertia Force.

Abstract: Advance of measurement system permits the measurement of high accuracy data. This study proposes analysis of shaft movement using this system. Firstly, we made a shaft model using finite element method and a club head model as concentrated mass. Secondly, we reduced amount of calculation by applying mode synthetics method. Input data for simulation is inertia force and torque calculated from swing data that is measured by motion capturing system and is treated data manually. Finally, we simulated shaft movement using these data, we could repeat shaft movement of face direction and toe direction.

## 1 INTRODUCTION

Golf is the sport that can enjoy valuable generation of people. Victory or defeat of this sport is decided by score that move a golf ball to fixed location. Therefore players want to get a golf club that is able to hit a golf ball more accuracy and more far for improving their playing. This study focuses on driver among some clubs because hitting with a driver determines score. For this reason, club head of driver was improved bigger and more reactive. However, not only volume of head of the golf club but also coefficient of the golf club was restricted by the effect rule of the spring of the United States golf society. Therefore, it is becoming hard to differentiate golf clubs for clubs spec. Then, the implementers of golf club increase the lineup of shaft and it provides the club fits for an individual. As one of techniques, "Database fitting" was established by SRI. "Database fitting" is the method that recommends adequate shaft to a player by analyzing the swing using grip end sensor.

In the future, the implementers would like to provide custom-made shaft for each golfer. In order to make this idea possible, the implementers need to repeat movement of shaft that don't exist in the lineup in swinging.

Some studies of prediction movement of shaft in swinging have using multi body dynamics (Inoue,

2000,2004), using vibration feature (Iwatsubo, 1990). However, the study using multi body dynamics needs huge amount of calculation because that has iterative calculation on that simulation. The study using vibration feature has smaller amount of calculation than multi body dynamics, but its simulation is calculated on 2-dimension and don't repeat realistic movement of shaft in swinging that need for its prediction.

Wherein, we intend to simulate movement of shaft by 3-dimension input data using motion capture system and by small amount of calculation applying mode synthetics method.

## 2 SIMULATION MODEL

Simulation model of shaft is constructed with multistage beam (Fig.1). Simulation model is formulated by finite element method with beam type element.

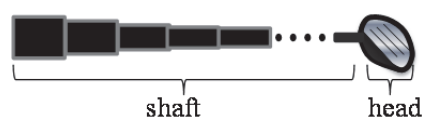


Figure 1: Simulation Model with Multistage Beam.

## 2.1 Beam Element

### 2.1.1 Displacement Function

Coordinate system of shaft is defined as Fig.2. In this study, x direction is defined as toe of club head direction and y direction is defined as face of club head direction. Displacement function of each directions on this coordinate system is shown in eq.(1), eq.(2).

$$x(z,t) = a_0 + a_1z + a_2z^2 + a_3z^3 \quad (1)$$

$$y(z,t) = b_0 + b_1z + b_2z^2 + b_3z^3 \quad (2)$$

Deflection and deflection angle of each direction of the  $i$ th element from grip end is defined as Fig.3, deflection and deflection angle of each direction is as follows.

$$x_{(i)} = a_0$$

$$\theta_{y(i)} = \left. \frac{dx(z,t)}{dz} \right|_{z=0} = a_1$$

$$x_{(i+1)} = a_0 - a_1L + a_2L^2 - a_3L^3 \quad (3)$$

$$\theta_{y(i+1)} = \left. \frac{dx(z,t)}{dz} \right|_{z=L} = a_1 - 2a_2L + 3a_3L^2$$

$$y_{(i)} = b_0$$

$$\theta_{x(i)} = \left. \frac{dy(z,t)}{dz} \right|_{z=0} = -b_1$$

$$y_{(i+1)} = b_0 - b_1L + b_2L^2 - b_3L^3 \quad (4)$$

$$\theta_{x(i+1)} = \left. \frac{dy(z,t)}{dz} \right|_{z=L} = -b_1 + 2b_2L - 3b_3L^2$$

$L$  is Element width. Each coefficients of eq.(1) and eq.(2) are derived from eq.(3) and eq.(4).

$$x(z,t) = [N_x(z)]\mathbf{d}_{x(i)}(t) \quad (5)$$

$$\mathbf{d}_{x(i)}(t) = [x_{(i)}, \theta_{y(i)}, x_{(i+1)}, \theta_{y(i+1)}]^T \quad (6)$$

$$[N_x(z)] = [N_{x1} \quad N_{x2} \quad N_{x3} \quad N_{x4}]$$

$$N_{x1} = 1 - 3\left(\frac{z}{L}\right)^2 - 2\left(\frac{z}{L}\right)^3$$

$$N_{x2} = L\left\{\left(\frac{z}{L}\right) + 2\left(\frac{z}{L}\right)^2 + \left(\frac{z}{L}\right)^3\right\} \quad (7)$$

$$N_{x3} = 3\left(\frac{z}{L}\right)^2 + 2\left(\frac{z}{L}\right)^3$$

$$N_{x4} = L\left\{\left(\frac{z}{L}\right)^2 + \left(\frac{z}{L}\right)^3\right\}$$

$$y(z,t) = [N_y(z)]\mathbf{d}_{y(i)}(t) \quad (8)$$

$$\mathbf{d}_{y(i)}(t) = [y_{(i)}, \theta_{x(i)}, y_{(i+1)}, \theta_{x(i+1)}]^T \quad (9)$$

$$[N_y(z)] = [N_{y1} \quad N_{y2} \quad N_{y3} \quad N_{y4}]$$

$$N_{y1} = 1 - 3\left(\frac{z}{L}\right)^2 - 2\left(\frac{z}{L}\right)^3$$

$$N_{y2} = -L\left\{\left(\frac{z}{L}\right) + 2\left(\frac{z}{L}\right)^2 + \left(\frac{z}{L}\right)^3\right\} \quad (10)$$

$$N_{y3} = 3\left(\frac{z}{L}\right)^2 + 2\left(\frac{z}{L}\right)^3$$

$$N_{y4} = -L\left\{\left(\frac{z}{L}\right)^2 + \left(\frac{z}{L}\right)^3\right\}$$

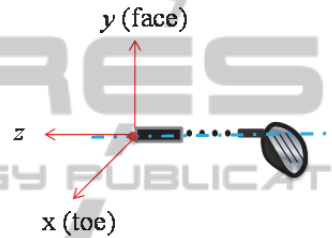


Figure 2: Coordinate System of Shaft.

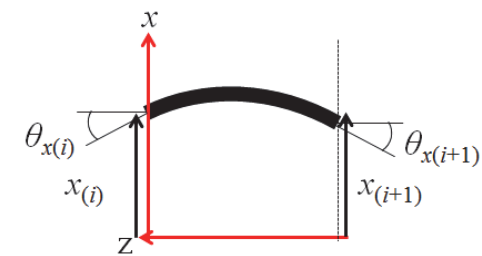
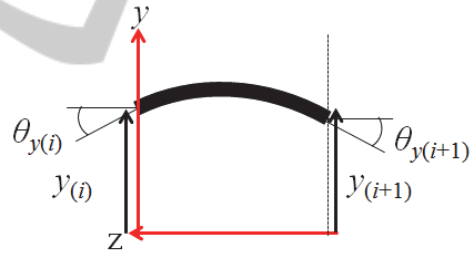


Figure 3: Each Deflection and Deflection angle.

### 2.1.2 Mass Matrix, Rigid Matrix

Motion energy of each directions  $T_x$ ,  $T_y$  and potential energy of each directions  $U_x$ ,  $U_y$  are led as following equations.

$$T_x = \int_{-L}^0 \rho A \left\{ \frac{dx(z,t)}{dt} \right\}^2 dz \quad (11)$$

$$T_y = \int_{-L}^0 \rho A \left\{ \frac{dy(z,t)}{dt} \right\}^2 dz \quad (12)$$

$$U_x = \int_{-L}^0 EI_x \left\{ \frac{d^2 x(z,t)}{dz^2} \right\}^2 dz \quad (13)$$

$$U_y = \int_{-L}^0 EI_y \left\{ \frac{d^2 y(z,t)}{dz^2} \right\}^2 dz \quad (14)$$

$A$  is cross-section area,  $\rho$  is density,  $E$  is Young's modulus,  $I_x$ ,  $I_y$  are second moment of area. By substituting eq.(5) and eq.(9) into eq.(11-14), we obtain element mass matrix of each directions as  $M_{ele\_x,y}$  and element rigid matrix of each directions as  $K_{ele\_x,y}$ .

$$M_{ele\_x,y} = \int_{-L}^0 \rho A [N_{x,y}(z)]^T [N_{x,y}(z)] dz \quad (15)$$

$$K_{ele\_x,y} = \int_{-L}^0 EI_{x,y} \left[ \frac{d^2 N_{x,y}(z)}{dz^2} \right]^T \left[ \frac{d^2 N_{x,y}(z)}{dz^2} \right] dz \quad (16)$$

Index  $x,y$  of eq.(15) and eq.(16) show each direction. By assembling these element matrixes, we compose full mass matrix and full rigid matrix.

## 2.2 Equation of Motion

In this study, simulation model of shaft is divided into 24 elements (Fig.1). By rearranging each element matrixes, the  $i$  th element equation of motion is composed as follows.

$$M_{(i)} \ddot{\mathbf{d}}_{(i)}(t) + C_{(i)} \dot{\mathbf{d}}_{(i)}(t) + K_{(i)} \mathbf{d}_{(i)}(t) = \mathbf{f}_{(i)} \quad (17)$$

$$\mathbf{d}_{(i)}(t) = [\mathbf{d}_{e(i)} \quad \mathbf{d}_{e(i+1)}]^T \quad (18)$$

$$\mathbf{d}_{e(i)} = [x_{(i)} \quad y_{(i)} \quad \theta_{x(i)} \quad \theta_{y(i)}]$$

$$\mathbf{d}_{e(i+1)} = [x_{(i+1)} \quad y_{(i+1)} \quad \theta_{x(i+1)} \quad \theta_{y(i+1)}]$$

Index  $(i)$  shows the  $i$  th node,  $\mathbf{f}_{(i)}$  is nodal force acting of the  $i$  th node,  $\mathbf{d}_{(i)}(t)$  is nodal point displacement,  $C_{(i)}$  is damping matrix. Mass of club head is added to final node as concentrated mass.

Then, substituting element mass matrix on final element as  $M_{(n)}$ , the element of  $M_{(n)}$  in the 1 row and 1 column and in the 2 th row and 2 column is as follow equations.

$$M_{(n)}(1,1) = M_{ele(n)}(1,1) - M_{head} \quad (19)$$

$$M_{(n)}(2,2) = M_{ele(n)}(2,2) - M_{head}$$

$M_{e(n)}$  is the element mass matrix led from eq.(5),

$M_{head}$  is mass of club head. By assembling each elements, full motion of equation is follow equation.

$$M\ddot{\mathbf{d}}(t) + C\dot{\mathbf{d}}(t) + K\mathbf{d}(t) = \mathbf{f} \quad (20)$$

## 2.3 Mode Synthetics Method

Simulation model of shaft is divided into two area that are  $c$  area and  $e$  area (Fig.4). By dividing its model area, nodal point displacement and mass matrix, rigid matrix are divided into each area. Then, reduction matrix  $[T_i]$  is calculated. By multiplying  $[T_i]$  from the front of eq.(20), eq.(20) is reduced to  $\mathbf{d}_c$  that shows area  $c$  and  $\xi$  that shows mode area (Nagamatsu, 1985).

$$[\tilde{M}] \begin{bmatrix} \ddot{\mathbf{d}}_c \\ \ddot{\xi} \end{bmatrix} + [\tilde{C}] \begin{bmatrix} \dot{\mathbf{d}}_c \\ \dot{\xi} \end{bmatrix} + [\tilde{K}] \begin{bmatrix} \mathbf{d}_c \\ \xi \end{bmatrix} = \{\tilde{\mathbf{f}}\} \quad (21)$$

$$[\tilde{M}] = [T_i]^T [M] [T_i]$$

$$[\tilde{C}] = [T_i]^T [C] [T_i]$$

$$[\tilde{K}] = [T_i]^T [K] [T_i]$$

$$\{\tilde{\mathbf{f}}\} = [T_i]^T \{\mathbf{f}\}$$

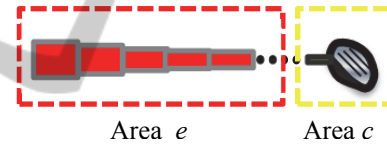


Figure 4: Dividing Simulation Model into Each Area.

## 2.4 Input Data

In this study, we model swing movement as 2-link model that is composed of arm and club for repeating shaft movement (Fig.5). Shaft is modelled by finite element method. Inertia force made by arm movement is added to shaft in swinging. Therefore, we need to calculate input data of this inertia force for repeating shaft movement. The method of calculating this input data is as follows.

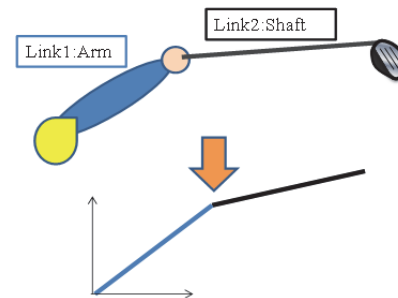


Figure 5: 2 Link Model of Swing.

### 2.4.1 Coordinate System

We define a shoulder shown on Fig.5 as origin point of inertial coordinate system  $[\mathbf{a}]$ . Then, we define the vector that shows from shoulder to shaft's point of union as  $\mathbf{r}_0$  and fixed coordinate system that origin point is its point of union as  $[\mathbf{b}]$ . We also define the vector that shows from this fixed coordinate system's origin point to the  $i$  th node as  $\boldsymbol{\rho}_{(i)}$ . And then, by defining movement by elastic deformation of the  $i$  th node as  $\mathbf{n}_{(i)}$ , the vector  $\mathbf{u}_{(i)}$  that shows from inertial coordinate system to the  $i$  th node obtains as follow.

$$\mathbf{u}_{(i)} = \mathbf{r}_0 + \boldsymbol{\rho}_{(i)} + \mathbf{n}_{(i)} \quad (22)$$

Each coordinate system and relationship of each vector is shown on Fig.6. The relationship of each coordinated system is obtained as follow.

$$[\mathbf{b}] = [\mathbf{a}]S \quad (23)$$

$S$  is coordinate transform matrix. Then, rate vector is obtained as follow by eq.(22).

$$\begin{aligned} \dot{\mathbf{u}}_{(i)} &= \mathbf{v}_{(i)} = \dot{\mathbf{r}}_0 + \dot{\boldsymbol{\rho}}_{(i)} + \dot{\mathbf{n}}_{(i)} \\ &= [\mathbf{a}]\dot{\mathbf{r}}_0 + [\mathbf{b}]\tilde{\omega}\boldsymbol{\rho}_{(i)} + [\mathbf{b}]\mathbf{v}_{n(i)} \end{aligned} \quad (24)$$

$\mathbf{v}_{n(i)}$  is component of rate vector of the  $i$  th node,  $\tilde{\omega}$  is angle rate tensor.

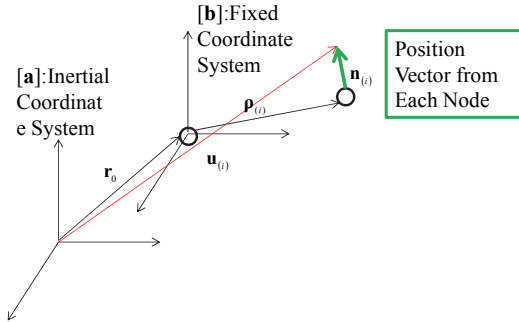


Figure 6: Each Coordinate System and Relationship of Each Vector.

### 2.4.2 Input Force

Gravity vector  $\mathbf{g}$  is shown by its component  $\hat{\mathbf{g}}$ .

$$\mathbf{g} = [\mathbf{a}]\hat{\mathbf{g}} \quad (25)$$

Then, we define linear momentum of the  $i$  th node as  $\mathbf{P}_{(i)}$  and obtain follow equation by law of conservation of liner momentum.

$$\dot{\mathbf{P}}_{(i)} = \langle \mathbf{g} \rangle \quad (26)$$

$\langle \rangle$  shows integral of mass. By substituting eq.(24)

into eq.(26), we obtain follow equation.

$$\begin{aligned} \frac{d}{dt} \langle ([\mathbf{a}]\dot{\mathbf{r}}_0 + [\mathbf{b}]\tilde{\omega}\boldsymbol{\rho}_{(i)} + [\mathbf{b}]\mathbf{v}_{n(i)}) \rangle &= \langle \mathbf{g} \rangle \\ [\mathbf{b}]\langle a_{n(i)} \rangle &= \langle \mathbf{g} \rangle - \frac{d}{dt} \langle ([\mathbf{a}]\dot{\mathbf{r}}_0 + [\mathbf{b}]\tilde{\omega}\boldsymbol{\rho}_{(i)}) \rangle \end{aligned} \quad (27)$$

$a_{n(i)}$  is the component of acceleration vector of the  $i$  th node on fixed coordinate system. Second on the right-hand side of eq.(27) is deformed as follow.

$$\begin{aligned} \frac{d}{dt} \langle ([\mathbf{a}]\dot{\mathbf{r}}_0 + [\mathbf{b}]\tilde{\omega}\boldsymbol{\rho}_{(i)}) \rangle \\ = \langle ([\mathbf{a}]\ddot{\mathbf{r}}_0 + [\mathbf{b}]\tilde{\omega}\dot{\boldsymbol{\rho}}_{(i)} + [\mathbf{b}]\dot{\tilde{\omega}}\boldsymbol{\rho}_{(i)}) \rangle \end{aligned} \quad (28)$$

Then, we deform eq.(28) by substituting eq.(23).

$$\begin{aligned} [\mathbf{b}]\langle a_{n(i)} \rangle &= \langle [\mathbf{b}]S^T\hat{\mathbf{g}} \rangle \\ - \frac{d}{dt} \langle ([\mathbf{b}]S^T\dot{\mathbf{r}}_0 + [\mathbf{b}]\tilde{\omega}\tilde{\omega}\boldsymbol{\rho}_{(i)} + [\mathbf{b}]\dot{\tilde{\omega}}\boldsymbol{\rho}_{(i)}) \rangle \\ \langle a_{n(i)} \rangle &= \langle S^T\hat{\mathbf{g}} \rangle \\ - \frac{d}{dt} \langle (S^T\ddot{\mathbf{r}}_0 + \tilde{\omega}\tilde{\omega}\boldsymbol{\rho}_{(i)} + \dot{\tilde{\omega}}\boldsymbol{\rho}_{(i)}) \rangle \end{aligned} \quad (29)$$

And then, by assuming inertia force that act to the  $i$  th node is composed by each next element, the first on the right-hand side of eq.(29) is explicated as follow equation.

$$\langle S^T\hat{\mathbf{g}} \rangle = \frac{1}{2}M_{(i)}S^T\hat{\mathbf{g}} + \frac{1}{2}M_{(i+1)}S^T\hat{\mathbf{g}} \quad (30)$$

In a similar way, the second on the right-hand side of eq.(29) is explicated as follow equation.

$$\begin{aligned} \frac{d}{dt} \langle (S^T\ddot{\mathbf{r}}_0 + \tilde{\omega}\tilde{\omega}\boldsymbol{\rho}_{(i)} + \dot{\tilde{\omega}}\boldsymbol{\rho}_{(i)}) \rangle = \\ \frac{1}{2}M_{(i)}(S^T\ddot{\mathbf{r}}_0 + \tilde{\omega}\tilde{\omega}\boldsymbol{\rho}_{(i)} + \dot{\tilde{\omega}}\boldsymbol{\rho}_{(i)}) \\ + \frac{1}{2}M_{(i+1)}(S^T\ddot{\mathbf{r}}_0 + \tilde{\omega}\tilde{\omega}\boldsymbol{\rho}_{(i+1)} + \dot{\tilde{\omega}}\boldsymbol{\rho}_{(i+1)}) \end{aligned} \quad (31)$$

Input force  $F_{(i)}$  of the  $i$  th node is led from eq.(29-31) as follow equation.

$$\begin{aligned} F_{(i)} &= \langle a_{n(i)} \rangle = \\ \frac{1}{2}M_{(i)}S^T\hat{\mathbf{g}} + \frac{1}{2}M_{(i+1)}S^T\hat{\mathbf{g}} \\ - \frac{1}{2}M_{(i)}(S^T\ddot{\mathbf{r}}_0 + \tilde{\omega}\tilde{\omega}\boldsymbol{\rho}_{(i)} + \dot{\tilde{\omega}}\boldsymbol{\rho}_{(i)}) \\ - \frac{1}{2}M_{(i+1)}(S^T\ddot{\mathbf{r}}_0 + \tilde{\omega}\tilde{\omega}\boldsymbol{\rho}_{(i+1)} + \dot{\tilde{\omega}}\boldsymbol{\rho}_{(i+1)}) \end{aligned} \quad (32)$$

Especially, by considering influence of club head, input force of final node is led as follow equation.

$$\begin{aligned}
 F \langle a_{n(i)} \rangle = & \\
 & \frac{1}{2} M_{(n)} S^T \hat{g} + M_{head} S^T \hat{g} \\
 & - \frac{1}{2} M_{(n)} \left( S^T \ddot{r}_0 + \tilde{\omega} \tilde{\omega} \rho_{(n)} + \tilde{\omega} \rho_{(n)} \right) \\
 & - M_{head} \left( S^T \ddot{r}_0 + \tilde{\omega} \tilde{\omega} \rho_{head} + \tilde{\omega} \rho_{head} \right)
 \end{aligned} \quad (33)$$

### 2.4.3 Input Torque

We define the  $i$  th node circular torque as  $\mathbf{T}_{(i)}$ .

$$\mathbf{T}_{(i)} = [\mathbf{a}] \hat{T}_{(i)} \quad (34)$$

$\hat{T}_{(i)}$  is component of the  $i$  th node circular torque on inertial coordinate system. Follow equations is led by low of conservation of angular momentum.

$$\langle \tilde{\rho}_{(i)} (\dot{\hat{v}}_{(i)} - \hat{g}) \rangle + \hat{T}_{(i)} = 0 \quad (35)$$

$$\hat{v}_{(i)} = \dot{r}_0 + S \tilde{\rho}_{(i)} \omega \quad (36)$$

$$\tilde{\rho}_{(i)} = S \tilde{\rho}_{(i)} S^T \quad (37)$$

$$\hat{T} = ST \quad (38)$$

$\tilde{\rho}_{(i)}$  is antisymmetrization tensor of fixed coordinate vector  $\rho_{(i)}$ . Follow equation is led by explicating eq.(38).

$$\langle \tilde{\rho}_{(i)} \dot{\hat{v}}_{(i)} \rangle + \hat{T} = \langle \tilde{\rho}_{(i)} \hat{g} \rangle \quad (39)$$

And then, the left-hand side of eq.(39) is explicated by eq.(36) and eq.(37) as follow equation.

$$\begin{aligned}
 \langle \tilde{\rho}_{(i)} (\dot{\hat{v}}_{(i)}) \rangle &= S \langle \tilde{\rho}_{(i)} \ddot{r}_0 \rangle + S \langle \tilde{\rho}_{(i)} \tilde{\omega} \tilde{\rho}_{(i)}^T \rangle \omega \\
 &+ S \langle \tilde{\rho}_{(i)} \tilde{\rho}_{(i)}^T \rangle \dot{\omega} \\
 &= S \langle \tilde{\rho}_{(i)} \ddot{r}_0 \rangle + S \langle \tilde{\omega} \tilde{\rho}_{(i)} \tilde{\rho}_{(i)}^T + \tilde{\rho}_{(i)} \tilde{\rho}_{(i)}^T \tilde{\omega} \rangle \omega \\
 &- (\rho_1^2 + \rho_2^2 + \rho_3^2) \tilde{\omega} \omega + SJ \dot{\omega} \\
 &= S \langle \tilde{\rho}_{(i)} \ddot{r}_0 \rangle + S \tilde{\omega} J_{(i)} \omega + SJ_{(i)} \dot{\omega}
 \end{aligned} \quad (40)$$

$$J_{(i)} = \langle \tilde{\rho}_{(i)} \tilde{\rho}_{(i)}^T \rangle \quad (41)$$

$$\dot{\hat{r}}_0 = S \ddot{r}_0 \quad (42)$$

$$\ddot{\hat{r}}_0 = S \ddot{r}_0 \quad (43)$$

$$\rho_{(i)} = [\rho_1 \quad \rho_2 \quad \rho_3]^T \quad (44)$$

Component of torque vector on fixed coordinate system is led by eq.(38-44) as follow equation.

$$T = -\langle \tilde{\rho}_{(i)} \ddot{r}_0 \rangle - \tilde{\omega} J_{(i)} \omega - J_{(i)} \dot{\omega} + \langle \tilde{\rho}_{(i)} \rangle S^T \hat{g} \quad (45)$$

In a similar way of input force, by assuming input torque is composed by each next element, each member of eq.(45) are explicated as follow equation.

$$\begin{aligned}
 T_{(i)} &= -\frac{1}{2} M_{(i)} \tilde{\rho}_{(i)} \ddot{r}_0 - \frac{1}{2} M_{(i+1)} \tilde{\rho}_{(i+1)} \ddot{r}_0 \\
 &- \frac{1}{2} \tilde{\omega} J_{(i)} \omega - \frac{1}{2} \tilde{\omega} J_{(i+1)} \omega - \frac{1}{2} J_{(i)} \dot{\omega} - \frac{1}{2} J_{(i+1)} \dot{\omega} \\
 &+ \frac{1}{2} M_{(i)} \tilde{\rho}_{(i)} S^T \hat{g} + \frac{1}{2} M_{(i+1)} \tilde{\rho}_{(i+1)} S^T \hat{g}
 \end{aligned} \quad (46)$$

Especially, by considering influence of club head, final node circular input torque is led as follow equation.

$$\begin{aligned}
 T_{(n)} &= -\frac{1}{2} M_{(n)} \tilde{\rho}_{(n)} \ddot{r}_0 - M_{head} \tilde{\rho}_{head} \ddot{r}_0 \\
 &- \frac{1}{2} \tilde{\omega} J_{(n)} \omega - \tilde{\omega} J_{head} \omega - \frac{1}{2} J_{(n)} \dot{\omega} - J_{head} \dot{\omega} \\
 &+ \frac{1}{2} M_{(n)} \tilde{\rho}_{(n)} S^T \hat{g} + M_{head} \tilde{\rho}_{head} S^T \hat{g}
 \end{aligned} \quad (47)$$

$\tilde{\rho}_{head}$  is the antisymmetrization tensor of the vector that shows from final node to center of mass of head,  $J_{head}$  is inertia moment of head.

## 3 ANALYSIS METHOD

### 3.1 Measurement

Shaft movement in swinging was measured by 3D motion capture system. Sampling frequency is 500[Hz], marker is attached on shaft as Fig.7. While, we define coordinate system for measurement as Fig.8.

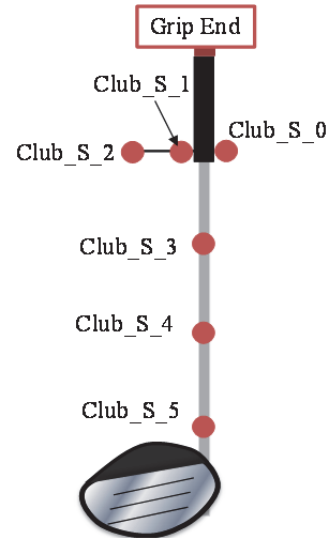


Figure 7: Marker Location.

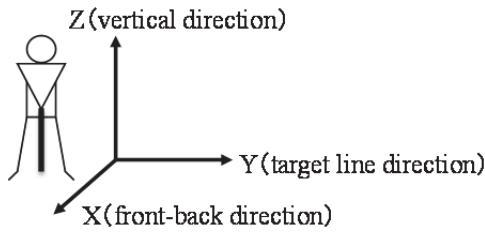


Figure 8: Coordinate System of Measurement.

### 3.2 Shaft Movement Prediction

Shaft movement was calculated by eq. (25) using newmark  $\beta$  method. We added damping as adequate numerical damping. Boundary condition was fixed end, input data was calculated by eq. (32-33) and eq. (46-47) using acceleration and angle rate, angle acceleration data that have been obtained from marker data of motion capture system. Acceleration was led using by filtered motion data and Euler's approach. Angle rate and angle acceleration data is led by quaternion. These programs were programed by Matlab.

## 4 RESULTS AND DISCUSSION

We show each direction's inertia force of shaft apex calculated by motion data on Fig.9 with face direction and Fig.10 with toe direction. And then, we show movement of each direction of marker S5 in close shaft apex on Fig.11 with vertical direction and front-back direction, on Fig.12 with vertical direction and target line direction. Blue line shows motion and red line shows simulation data. Red asterisk of Fig. (11-12) shows top of marker position in swinging and lime green asterisk of Fig. (11-12) shows the moment of impacting golf ball. By showing Fig.11, there is the difference of about 0.035[m] motion line and simulation line near top. However, by showing near impacting on Fig.11, there is shorter difference of about 0.015[m] motion line and simulation line near the moment of impacting golf ball. Then, by showing Fig.12, there is the difference of about 0.04 [m] motion line and simulation line near top. However, by showing near impacting on Fig.12, there is shorter difference of about 0.015[m] motion line and simulation line near the moment of impacting golf ball. For all of these reasons, we concluded that we could repeat shaft movement in swinging using by this simulation model.

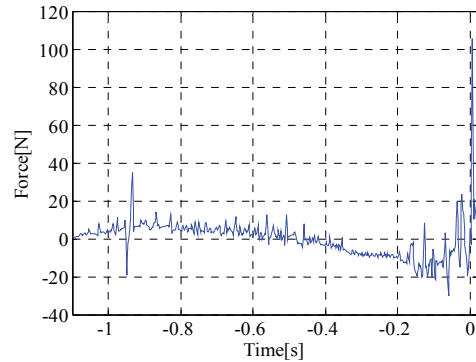


Figure 9: Inertia Force of Face Direction.

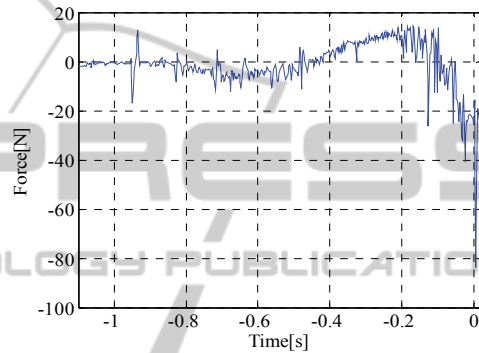


Figure 10: Inertia Force of Toe Direction.

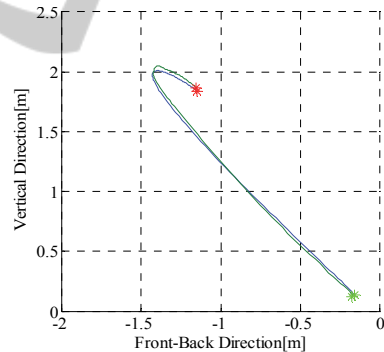


Figure 11: Position Data as Viewing from behind target line direction.

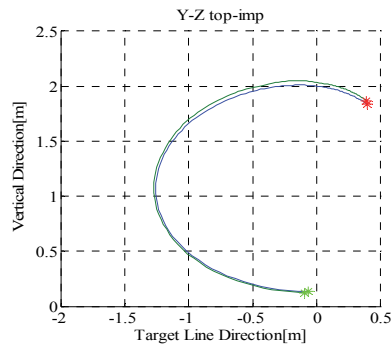


Figure 12: Position Data as Viewing from front - front-back Direction.

## 5 CONCLUSIONS

In this study we modelled shaft by finite element method. And then, we reduced amount of calculation by applying mode synthetics method and simulation model calculated input data for this model from motion data. By using this simulation model and input data, we concluded that we could repeat shaft movement in swinging using by this simulation model.

## REFERENCES

- Yoshio Inoue, Yoshihiro Kai, Tetsuya Tanioka, 2000, Study on Dynamics of Golf Swing (Boundary Condition and Elasticity of Shaft), *the Japan Society of Mechanical Engineering*
- Yoshio Inoue, Kyoko Shibata, Koichi Okayama, Kyoji Totsugi, 2004, Effect of the shaft elasticity in golf swing, *the Japan Society of Mechanical Engineering*
- Takuzo Iwatsubo, Nobuki Konishi, Tetsuo Yamaguchi, 1990, Research on Optimum Design of a Golf Club, *the Japan Society of Mechanical Engineering*
- Akio Nagamatsu, 1985, Mode Analysis, *baihukan*, 4<sup>th</sup> edition, pp.215-216